Prabha Materials Science Letters
Vol. 3, No. 1, 29-45, 2024
https://doi.org/10.33889/PMSL.2024.3.1.002

Ram Arti Publishers

Nanostructuring of Ferritic Steel: A Review on Enhanced Surface Properties Using Ultrasonic Shot Peening

Ankitendran Mishra
Department of Metallurgical Engineering,
Indian Institute of Technology (BHU), Varanasi, Uttar Pradesh, India.
Corresponding author: mishra.ankitendran@gmail.com

Ankita Ojha
Department of Chemistry,
Maharaja College, Arrah, Bihar, India.
E-mail: ankitaojha1208@gmail.com

(Received on April 17, 2023; Revised on July 26, 2023 & October 10, 2023; Accepted on October 25, 2023)

Abstract
Nanostructuring of ferritic stainless steel refers to the process of intentionally reducing the grain size of the material at the nanoscale level. By manipulating the microstructure of the steel, it is possible to enhance its mechanical, physical, and chemical properties. Nanostructuring can significantly improve the strength, hardness, and wear resistance of ferritic stainless steel, while still maintaining its corrosion resistance. The increased density of grain boundaries and the complex dislocation network within the nanostructured material contribute to these improved properties. Moreover, the nanostructured ferritic stainless steel exhibits enhanced thermal stability, leading to better high-temperature performance and resistance to creep deformation. The small grain size also allows for increased precipitation of secondary phases, such as carbides, nitrides, or intermetallic compounds, which can further improve the material's properties. There are several methods to achieve nanostructuring in ferritic stainless steel, such as severe plastic deformation (SPD) techniques like high-pressure torsion, equal channel angular pressing, and accumulative roll bonding. These techniques impose extreme plastic deformation on the material. Leading to grain refinement below the micrometre range. Also, a novel method of surface nanostructuring ultrasonic shot peening (USP) is discussed in detail.

Shot peening is a process in which small, spherical media, typically made of steel or ceramic, called "shots," are propelled onto the surface of a material at high velocities. Ultrasonic shot peening enhances the traditional shot peening process by introducing high-frequency vibrations to the shots. These vibrations are generated by an ultrasonic transducer, which is immersed in a bath of shots and liquid. The vibrations are transmitted through the liquid to the shots, causing them to collide with the surface of the ferritic steel at even higher velocities and energy levels than in traditional shot peening. In summary, nanostructuring of ferritic stainless steel offers great potential for tailoring the material's properties to meet specific application requirements, including improved strength, hardness, wear resistance, corrosion resistance, and high-temperature performance. USP is an effective surface treatment method for ferritic steel, offering advantages in terms of fatigue life, stress corrosion cracking resistance, surface hardness, and wear resistance.

Keywords- Ferritic steel, High temperature corrosion, Erosion, Corrosion-erosion, Surface modification, Nanostructuring.

1. Introduction

Ferritic stainless steel is a low maintenance material with large endurance. They have appreciable cost to life advantage over other grades of carbon steels. In the present scenario, 60% of newly developed stainless steels are recycled from melted scrap (Reck et al., 2010). Apart from recyclability and low cost, these steels possess several appealing countenances like strong corrosion-resistance, creative appearance, heat resistance, biological neutrality, and uncomplicated fabrication. These characteristics of stainless steel are clearly displayed in Ferritic stainless steel which is a member of the stainless steel family. These steels contain higher chromium content ranging from 10.5 to 30 wt% and possess properties superior to austenitic steels on several occasions. The Fe–C–Cr diagram along 18% chromium, shown in Figure 1, indicates that

the austenite is not possible to form until a very high temperature (1200 ℃) is attained for the low carbon content of 0.06%.

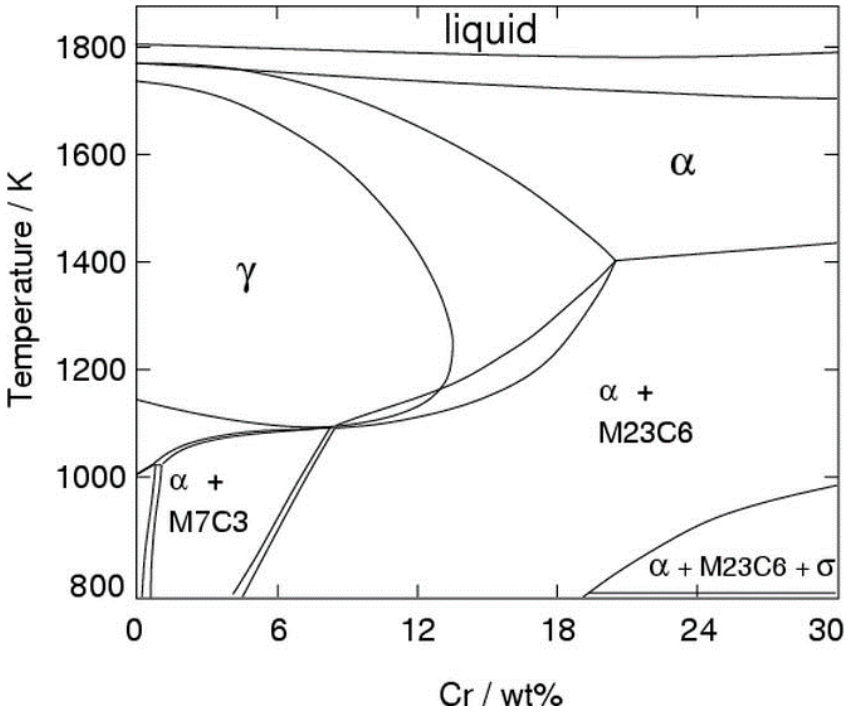

Figure 1. Fe-Cr-C phase diagram [Reprinted from Kubaschewski (2013), *Iron—Binary phase diagrams*. Springer Science & Business Media, 31-34].

This leads to the fact that steel of this composition is ferritic from room temperature till 1200 ℃ and is not susceptible to hardening. The ferritic steels are extremely superior to low-carbon steels in annealed conditions. They are fairly stronger with soft and ductile character and carry good forming ability at the same time.

1.1 Structure and Constitution of Ferritic Stainless Steel

Ferritic stainless steel is chromium-rich (α) solid solution having a body-center-cubic crystal (BCC) structure with thinly dispersed carbide in the microstructure, at room temperature. Figure 2 shows the iron-chromium binary equilibrium phase diagram for ferritic stainless steel. These steels have magnetic properties and have fewer slip systems, which lowers the plastic formability under plastic deformation.

Ferritic stainless steel is accessible in five different grades and acquires 25-40% of the total production of stainless steel. Some of these are classified as standard grades (Groups 1, 2 and 3) and some as special grades (Group 4 and 5). Table 1 shows the classification of these steel grades. The lowest chromium content forms Group 1 while Group 2 with high chromium content is the most commonly used grade. They have high corrosion resistance and fulfil the purpose of replacing austenitic Grade 304.

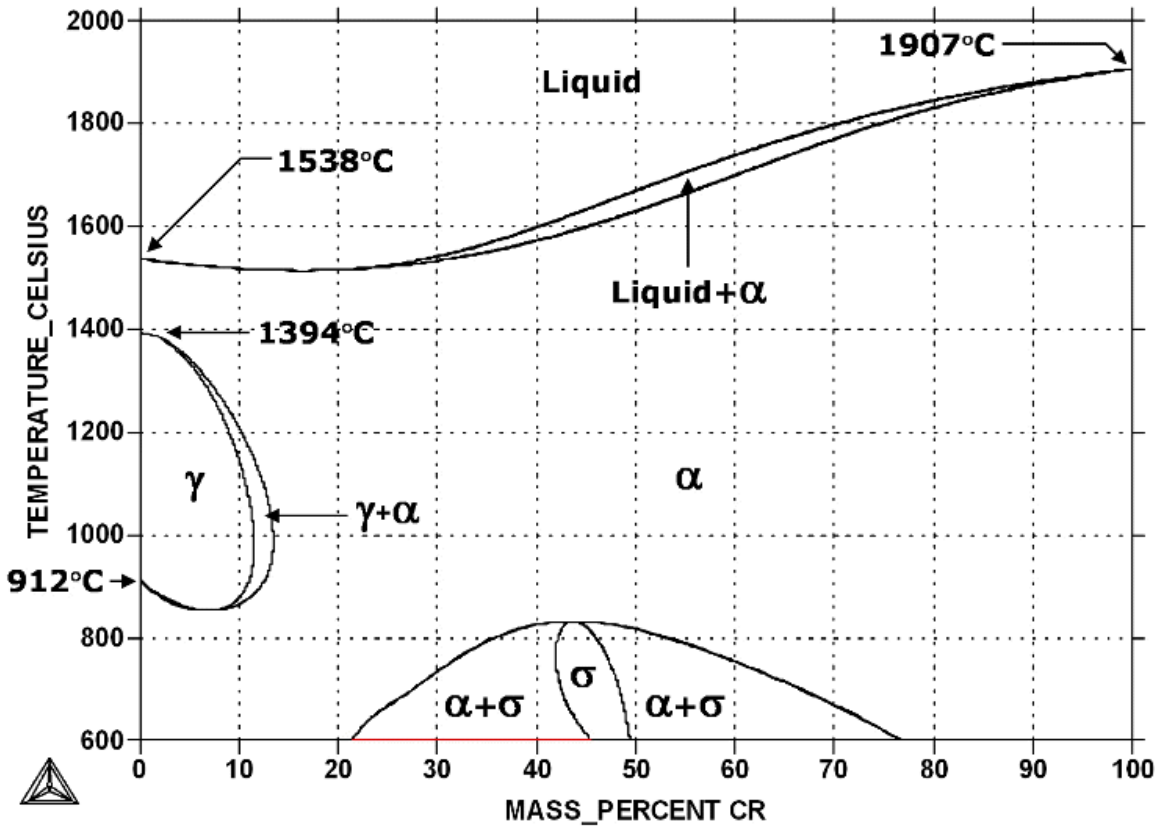

Figure 2. Iron-chromium binary equilibrium phase diagram. from Kubaschewski (2013), *Iron—Binary phase diagrams*. Springer Science & Business Media, 31-34].

The Group 3 ferritic steel with chromium content up to 18 wt% has better welding and forming ability. The special grade ferritic steels of Group 4 has higher chromium with a higher Mo concentration of nearly 0.5wt%, while Group 5 has chromium in the range of 25-30wt% and Mo may increase up to 3wt%. This special grade ferritic steels with more than 20wt% chromium do not generally form austenite at any temperature and are called as "Superferritic grades".

Type AISI 446 stainless steel has excellent oxidation resistance at elevated temperatures, high thermal conductivity, higher yield strength than austenitic stainless steels, and lower tensile ductility. In terms of corrosion resistance, these steels are preferable to martensitic stainless steel. Super ferritic steels such as Type AISI 446 stainless steel is included in ASTM specifications A176-74 (Chromium stainless flat products), A511 (Seamless stainless steel mechanical tubing), A268-74 (Ferritic stainless steel tubing for general service) and also in ASME code and AISI and SAE specifications.

1.2 Effects of Alloying Elements

The stability of ferritic stainless steel is largely dependent upon the ferrite and austenite phase stabilizing elements. The modified Schaffler's diagram (Figure 3) predicts the structure of stainless steel based on Ni and Cr equivalent. The general effect of alloying elements in ferritic steels are as follows:

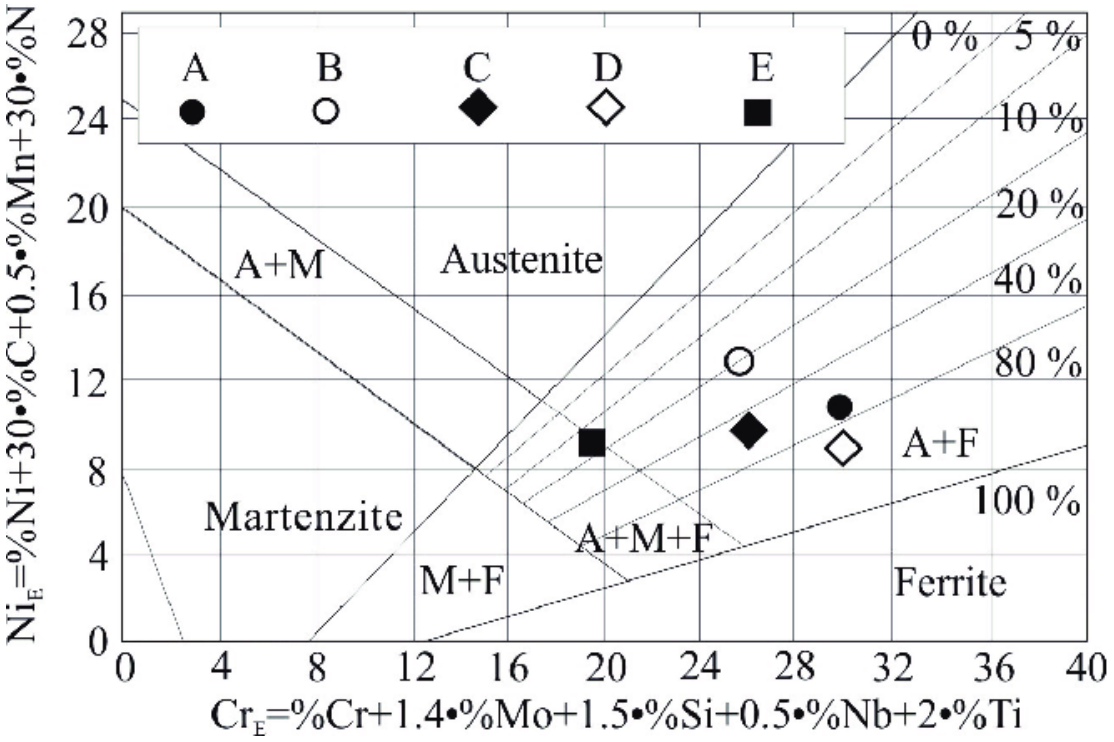

Figure 3. Modified Schafflers diagram [Reprinted from Charles et al., 2009, *Revue de Métallurgie*, *106*(3), 124-139].

Table 1. Classification of Ferritic stainless steel on the basis of chromium content and their market share.

Classification	Groups	Chromium wt%	Market share	Specific types
Standard ferritic grade	Group1	10-14	30 %	Type 409, 410, 420
	Group2	14-18	48 %	Type 430
	Group3	14-18 stabilized	13 %	Type 430 Ti, 441 with stabilizing elements like Ti, Mo etc.
Special ferritic grade	Group4	10-18 + 0.5% Mo	7 %	Type 434, 436, 444
	Group5	18-30	2 %	Type 445, 446, 447

***Carbon*:** The majority of the carbon present appears as finely divided chromium carbide precipitates. The addition of carbon shows two effects on the phase diagram. Firstly, the narrow region of the two-phase field γ + α is expanded by shifting the austenite phase boundary towards higher chromium content. Also, this γ + α two-phase field is shifted to a higher temperature. Secondly, the solubility of carbon being low in the α-matrix is rejected from a solid solution as complex carbides, which precipitates predominantly at the grain boundary. The Group 5 grade steel such as 446, 445 and 447, contains extra low carbon as interstitials to ensure sufficient structural stability.

***Nitrogen*:** Nitrogen also acts as a powerful γ + α two-phase field expander. It complements the strength by forming an interstitial solid solution and retards the embrittlement by precipitation of sigma (σ) phase. Nitrogen occupies octahedral sites where lesser strain energy is required. The number of octahedral sites being low in the case of BCC structure, the solubility of nitrogen in ferritic steel is very low. Thus, extra nitrogen precipitates out to form Cr_2N which increases its resistance to localized corrosion.

***Chromium*:** Chromium is a member of the group of ferrite phase stabilizers. It suppresses the gamma phase field and extends the sigma phase field. Beyond 13 wt% chromium, the transformation from α to γ is no longer possible. The superferritics having low interstitials and high chromium remains BCC throughout from room temperature to melting point and therefore, grain refinement and hardening by heat treatment and quenching are no longer possible.

***Manganese*:** Similar to Cr, segregation of impurities at the grain boundaries is improved. It also replaces Ni to some extent and induces temper embrittlement. Manganese depresses the transformation from γ to α phase at lower temperatures.

***Molybdenum*:** Improvement in pitting and crevice corrosion is achieved by Mo alloying. It is a distinct carbide former and ferrite phase stabilizer. Mo addition can produce fine-grained steels, improved fatigue strength, and delayed temper embrittlement. It also improves nitrogen solubility on one hand but increases the sigma phase formation tendency too.

The Group 5 stainless steel has a chromium range of 25-30% and extremely sensitive to embrittlement due to precipitation of the intermetallic phase. Their uses are restricted to thin gauges as they are very difficult to weld. The high chromium and molybdenum containing grades are known as 'Superferritics'. These new generation grades of ferritic steel are designed to have an extra-low interstitial content, thereby, further diminishes the possibility of intermetallic phase (sigma and chi) precipitation. Replacing titanium in applications undergoing severe corrosion, like condensers and heat exchanger tubes, is another rationale for the development of these super ferritic steels. Erosion backed by hot-corrosion is a common phenomenon that causes the failure of heat exchangers, boilers and pressure vessels used in coal-fired power generation units. An accelerated attack of oxidation of structural component commonly called as 'Hot Corrosion' occurs by deposition of Na_2SO_4 on a metal surface at high-temperature in range of 700-900°C (Hancock, 1987**)**. When sodium chloride laded breeze in conjunction with sulphur entrained in fuel deposits on the hot-section component, the degradation of the surface takes place causing severe loss of the material from the inner surface of the generation units.

1.3 Application of Ferritic Steels

The application of ferritic stainless steels is gaining importance due to their physical, chemical and mechanical properties. Along with, they also have strong corrosion and oxidation resistance, and excellent resistance to crevice, pitting and stress corrosion cracking. These properties makes the material viable to certain corrosion applications like heat exchangers, food industries and architectural trims, etc. The

pipelines of the heat exchangers during their operation and maintenance undergo hot corrosion due to salt present in the flowing fluid. The presence of this salt in high-temperature conditions causes hot corrosion, which degrades the material surface and enhances the erosion rate. Type AISI 446 stainless steel are high-chromium ferritic steels having excellent resistance to general, intergranular and pitting corrosion and stress corrosion cracking which makes it suitable for a wide variety of applications charged with chlorides, organic acids, and chloride stress-corrosion environment such as heat exchanger tubing, feed-water tubing and in equipment that operates with chloride-bearing or brackish cooling waters.

This class of stainless steel is substituting the austenite steels from various prominent applications as they offer a host of other technical, aesthetic and practical advantages and the application spectrum of ferritic steel covers variable sectors of the industrial world. The potential application of these steels are limitless depending upon the grades and composition. The enormous application of these steels with grade specific details is enlisted in the Table 2 below.

Table 2. Application of steels with their representative groups.

Groups	Representative Grades	Product Form	Application
1	Types 409,410,420	Strips, sheets, cold rolled bars/rods, tubes and pipes, etc.	Catalytic converter, thermostat, paddle wheel, washing machine drums, roof support structure.
2	Type 430		Condenser, cracking unit of petrochemical, train carriages, bus frames, kitchen extractor hood, urban furniture.
3	Types 430Ti, 441 with stabilization elements Ti, Nb, Mo		Boilers, foods, home and office equipment, building and civil construction, urban infrastructure.
4	Types 434, 436,444 with Mo>0.5%		Cladding of building, supports for lifts/ escalators, conveyor belts, drinking water pipelines, supports for photovoltaic cells.
5	Types 445, 445J1, 445J2, 446, 447		Heat exchangers, boilers, hot water tank, floors, mufflers, hydrogenation plant parts, super heater pipelines, annealing enclosures.

Applications of ferrtic steel as limited by corrosion-erosion (Koul and Castillo, 1993; Prakash, 2008; Zheng et al., 1995). Mechanical damage caused due to tube fretting and wear, fatigue cracking and erosion-corrosion cause operational difficulty (Chung et al., 2021; Chung et al., 2023; Wang et al., 2022a; Wang at al., 2022b). This provided ample scope to the researchers for developing numerous strategies for corrosion resistance. In this review, these strategies are depicted in brief.

2. Methods to Mitigate Erosion and Increase Corrosion Resistance of the Materials

High-temperature oxidation and erosion by the impact of fly ash and unburnt carbon particles are a few serious problems that need to be addressed in heat exchangers tubes, power plant boilers, etc. Different protective methods being used to mitigate the wastage arising out of the synergetic effect of erosion and corrosion include:

- Strengthening Mechanism
- Protective coatings for erosion
- Surface treatment for grain refinement.

2.1 Strengthening Mechanism

Like cold working, grain size hardening and solid solution strengthening available for single-phase materials are effective in improving the erosion resistance of eroding materials.

Table 3. Effect of various strengthening mechanism on the room temperature erosion of single-phase material (Sundararajan and Roy, 1997; Kumar et al., 2023).

Mechanism of hardening	Test material	Concluding remark
Annealed pure metal	Pure metals Al, Ni, Cu, Zr	Good correlation between erosion rate and both annealed hardness and melting point
Dislocation strengthening (cold work)	Pure metals Cu, Ni	Erosion resistance was either unaffected or deteriorated with increased cold work
Grain size hardening	304SS, Al, Fe, Fe Cu, Ti	The erosion rate was essentially independent of grain size. Fine-grained Fe was the only exception.
Solid solution strengthening	Cu, Cu-Zn, Cu-Al Ni, Ni-Cr 304SS and 316SS	Solid solution strengthening reduced erosion resistance in Cu-base alloy. Solid solution strengthening improved erosion resistance in Ni-based alloy.

Even in multiphase alloys, strengthening mechanism results in substantial improvement in materials strength but the erosion resistance changes only marginally. In the case of intermetallic, erosion rate is seen to be lower than the base material but the erosion rates of various intermetallic are comparable in spite of their varying crystal structure and melting point. Table 3 shows a wide variety of quenched and tempered steel that has been studied to characterize their erosion behavior. McCabe et al. (1985) concluded that spheroidized steel exhibited a minimum erosion rate while martensite microstructure showed maximum erosion rate. Pearlite and tempered martensite have intermediate erosion rates. Kumar et al.(2021) have studied the erosion behaviour of pre-oxidized high manganese nitrogen stabilized austenitic stainless steel and concluded that the erosion is rate strongly depends upon alloy composition.

2.2 Protective Coatings for Erosion

Although different types of coating techniques are available, however, from economic as well as availability point of view the methods shown in Figure 4 are currently used.

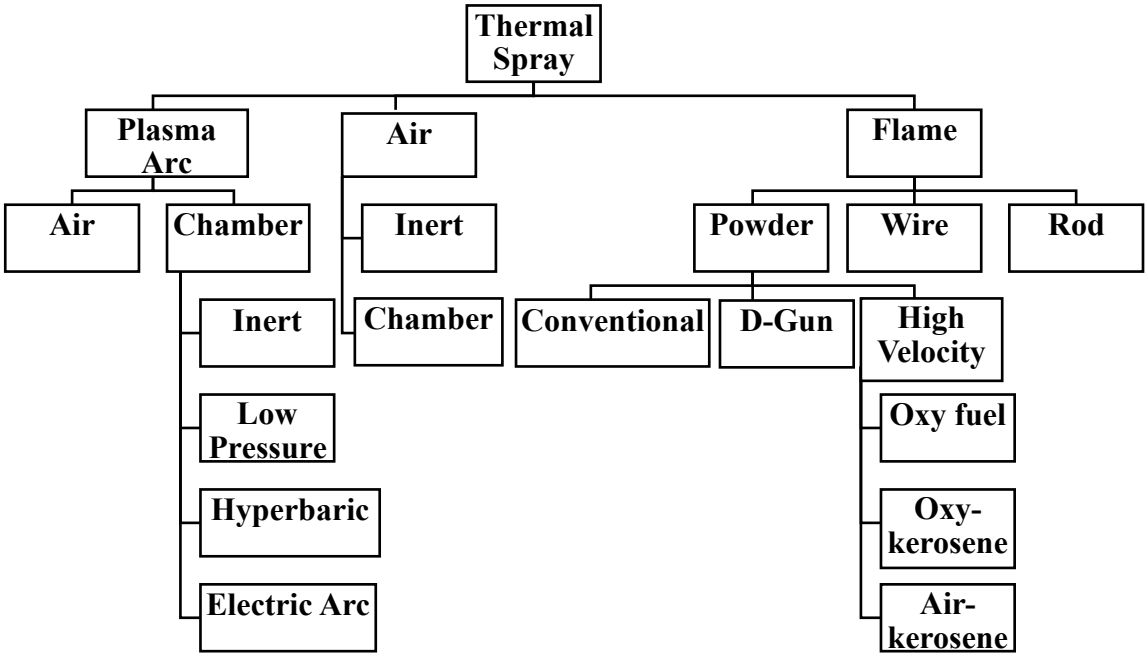

Figure 4. Classification of the thermal spray coating process [Reprinted with permission from Mishra, 2019].

2.3 Surface Treatments for Grain Refinement

Nanostructured materials possess superior mechanical and physical properties, improved corrosion resistance, and higher wear resistance. The nanostructured surface is synthesized using two complementary approaches

- **"Top-down" approach:** the existing coarse-grained materials are processed to achieve grain refinement and nanostructure, involving large plastic deformation, in which materials are subjected to large plastic deformation**.**
- **"Bottom-up" approach:** in which nanostructured materials are assembled from individual atoms or from nanoparticles.

Numerous techniques are developed to form surface nanostructure. Some of them are listed as are ultrasonic shot peening (USP)/surface mechanical attrition treatment (SMAT), laser shock peening, hammer peening, surface rolling, and high-speed drilling. These surface treatments introduce compressive residual stress along with refining themicrostructure in the surface region of the components. Ultrasonic shot peening (USP) induces compressive residual stress to larger depth and also refines the microstructure of the surface region even up to nanoscale.

3. Ultrasonic Shot Peening (USP) – A Novel Approach To Produce Surface Nanostructure

Apart from various discussed techniques, surface modification is the most promising route to enhance the erosion-corrosion behavior of materials substrate. Several processes of surface modifications and microstructure development, like, severe plastic deformation, surface coatings, ball milling, shot peening, friction stir processing, LSP and USP takes the advantage to intensify the surface properties of the structural component (Balakrishnan et al., 2008; Dwivedi et al., 2023; Qiz et al., 2023; Rai et al., 2014; Yue et al., 2002). In general, plastic deformation techniques have proved to be instrumental in modifying the corrosion resistance of the metallic material. USP is a relatively new technique of grain refinement that significantly improves the mechanical properties of metallic materials by inducing compressive residual stress through ball impact over the surface and brings no change to their chemical composition (Kumar et al., 2014; Sanda et al., 2011). Figure 5 shows a schematic representation of the USP process.

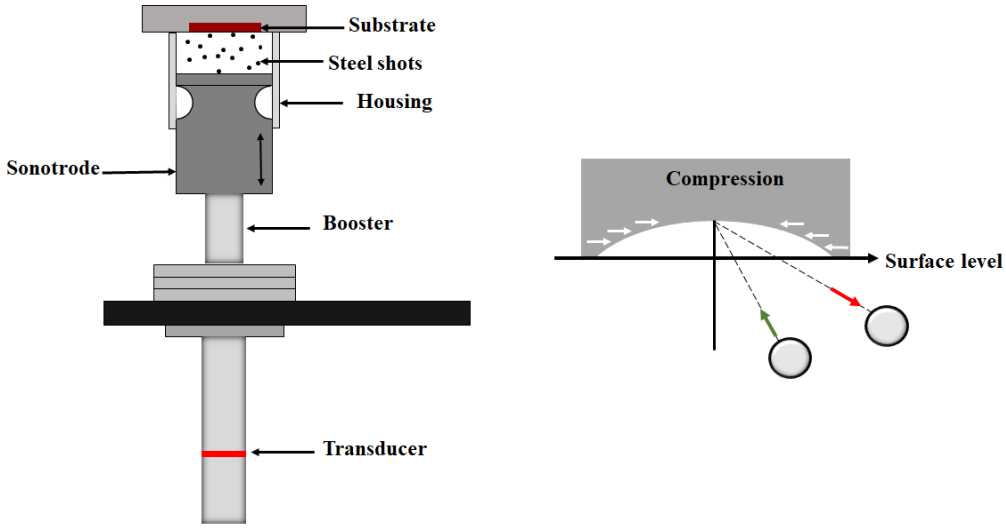

Figure 5. Schematic showing the principle of ultrasonic shot peening.

The impacting balls in Figure 5 act as a hammer creating indentation or semi-sphere, thereby increasing the hardness of the surface. USP generates grain refinement along with other defects which provide a short-circuit path for the diffusion of beneficial solute atoms at the free surface and create a protective oxide layer (Oka et al., 1997; Tan et al., 2008). The compressive residual stresses developed in the surface and sub-surface regions together with grain refinement increase the corrosion resistance and thus, the life span of the component (Chen et al., 2014; Lee et al., 2009). Under the effect of USP treatment, the rapid diffusion of chromium ions along grain boundaries as compared to through grain themselves improves the corrosion and oxidation properties of ferritic steel (Fragoudakis et al., 2013; Peltz et al., 2014). The corrosion nature of materials with modification in superficial properties is a promising area to explore (Mishra and Balasubramaniam, 2004;Wang et al., 2007). The corrosion rate increases two folds in the presence of erosion, which is responsible for generating flakes on the surface under the repeated impact of the particle (Li et al., 1995). Hot corrosion resistance is improved by USP (Kumar et al., 2016; Pradhan et al., 2018). The effect of USP on hot corrosion-erosion behavior of high chromium ferritic steel is hardly investigated and reported.

3.1 Effect of Ultrasonic Shot Peening on Surface Microstructure

It is important to understand the mechanism of surface nanostructuring from ultrasonic shot peening. Due to gradient in strain and strain rate from the treated surface to the substrate, a gradual increase occurs in grain size, from a few nanometers to several micrometers without any sharp interface.

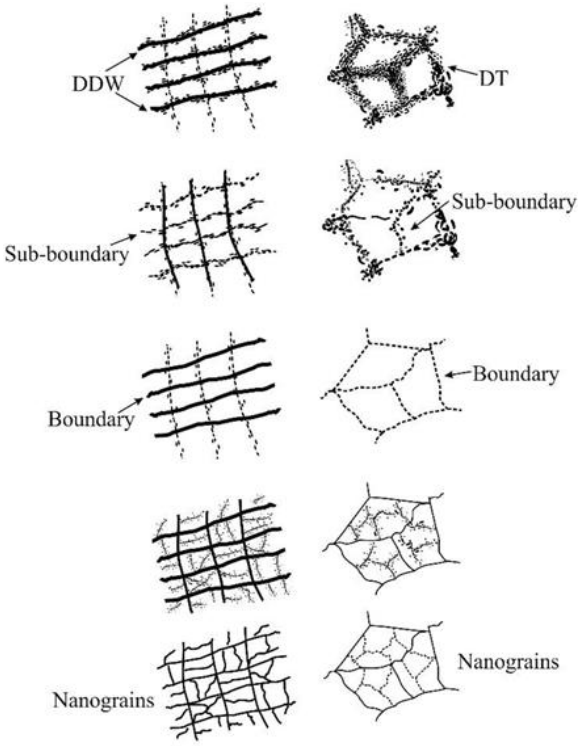

Figure 6. Schematic illustration of grain refinement via DDW and DT [*Reprinted from* Tao et al., 2008, Materials science forum, Vol. 579, pp. 91-108 *with permission from* Trans Tech Publications Ltd.].

Several studies have been carried out to characterize the modified microstructure from surface to substrate in different metals and alloys (Liu et al., 2000; Pandey, 2018; Roland et al., 2006; Sun et al., 2007; Wang

et al., 2005; Wang et al., 2006; Wang et al., 2003; Zhu et al., 2004). The plastic deformation and dislocation activities in metals and alloys strongly depends on their crystal structure and stacking fault energy (SFE). Therefore, this technique can be widely used for all ferritic and austenitic stainless steel, and other metals and alloys. (Bao et al., 2022; Chen et al., 2021; Chen and Zhang, 2021; Chen et al., 2023; Rehman et al., 2023; Yang et al., 2022; Yue et al., 2022).

Broadly, grain refinement mechanism of metals are categorized based on their SFE. In metals with high SFEs, dislocation walls and dislocation cells are developed to accumulate strains and consequently sub-boundaries are formed on further straining to subdivide the coarse grains. On the other hand, in metals of low SFEs, plastic deformation mode may shift from dislocation slip to mechanical twins under high strain rates and low temperature. Iron is a metal with high SFE of about 200 mJ/m^2 as shown in Figure 6. firstly formation of dense dislocation walls (DDWs) and dislocation tangles (DTs) occurs and subsequently these DDWs and DTs transform into sub-boundaries and get divided into smaller grains. Further straining leads to formation of nanostructure with high misorientation.

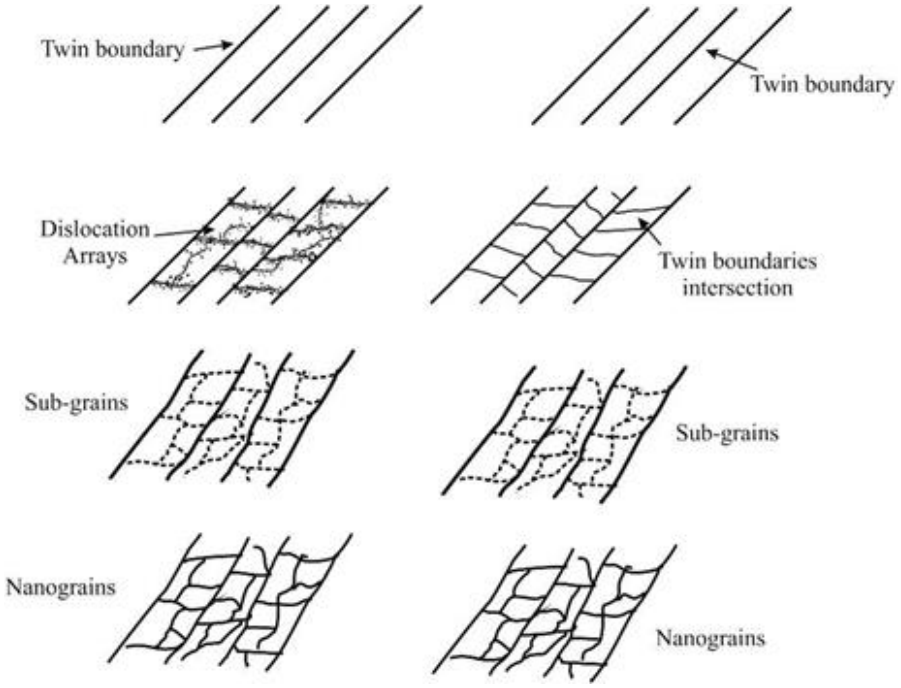

Figure7. Schematic representation of grain refinement by mechanical twins and dislocation resulting from SMAT [*Reprinted from* Tao et al., 2008, Materials science forum, Vol. 579, pp. 91-108 *with permission from* Trans Tech Publications Ltd.].

AISI 304 stainless steel has very low SFE of 17 mJ/m^2, instead of DDWs as in iron, there is formation of planar arrays of dislocations and twins on {111} slip planes of austenite phase (Zhang et al., 2003). Increase in strain results in interaction of twins which leads to further division of austenite grains into refined blocks (Figure 7). Formation of martensite phase is observed at interaction of twins.

For HCP and FCC metals (Pandey, 2018; Zhu et al., 2004), with low stacking fault energy, high density parallel twins are formed to divide the coarse grains into lamellar twin/matrix alternate blocks. On increasing strain twin-twin interactions leads to division of the grain into rhombic blocks and result into nanometer sized crystallites with large angle boundaries.

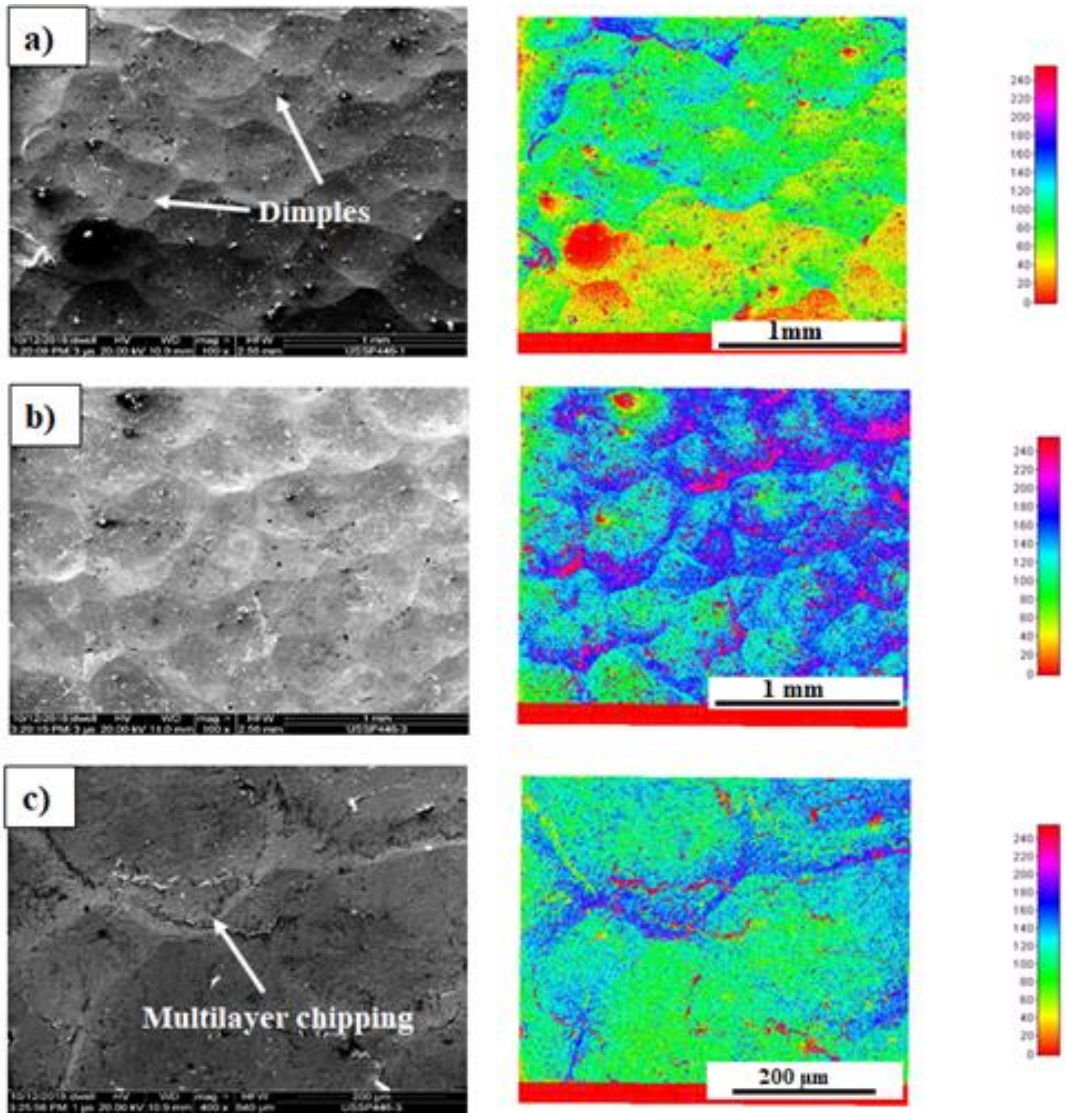

Figure 8. The optical micrograph shows that the effect of shot peening (a) 1 min USPed (b) 2 min USPed (c) 3 min USPed. [*Reprinted from* Mishra et al., 2020, Engineering Failure Analysis, 118, 104873 *with permission from* Elsevier.

The ultrafine-grained microstructures in the surface layer of Type AISI 446 Stainless Steel subjected to USP treatment was studied by (Mishra et al., 2020). The optical micrograph in Figure 8 shows that the effect of shot peening leads to grain refinement to a depth of ~175 µm. The average roughness (R_a) illustrates that the R_a value for the non-USP surface is lesser than the USP surface. Bright-field TEM micrograph of the Type AISI 446 Ferritic steel sample shows primary phase ferrite with some retained austenite. Also, some carbides precipitates are seen (Figure 9 (a,b)). The bright-field TEM micrograph of the USPed sample shows a high density of dislocation labyrinth within the grain. The ring-type pattern in selected area diffraction (SAD) acknowledges the refinement of original coarse grain to nanograins (Figure 9 (c,d)).

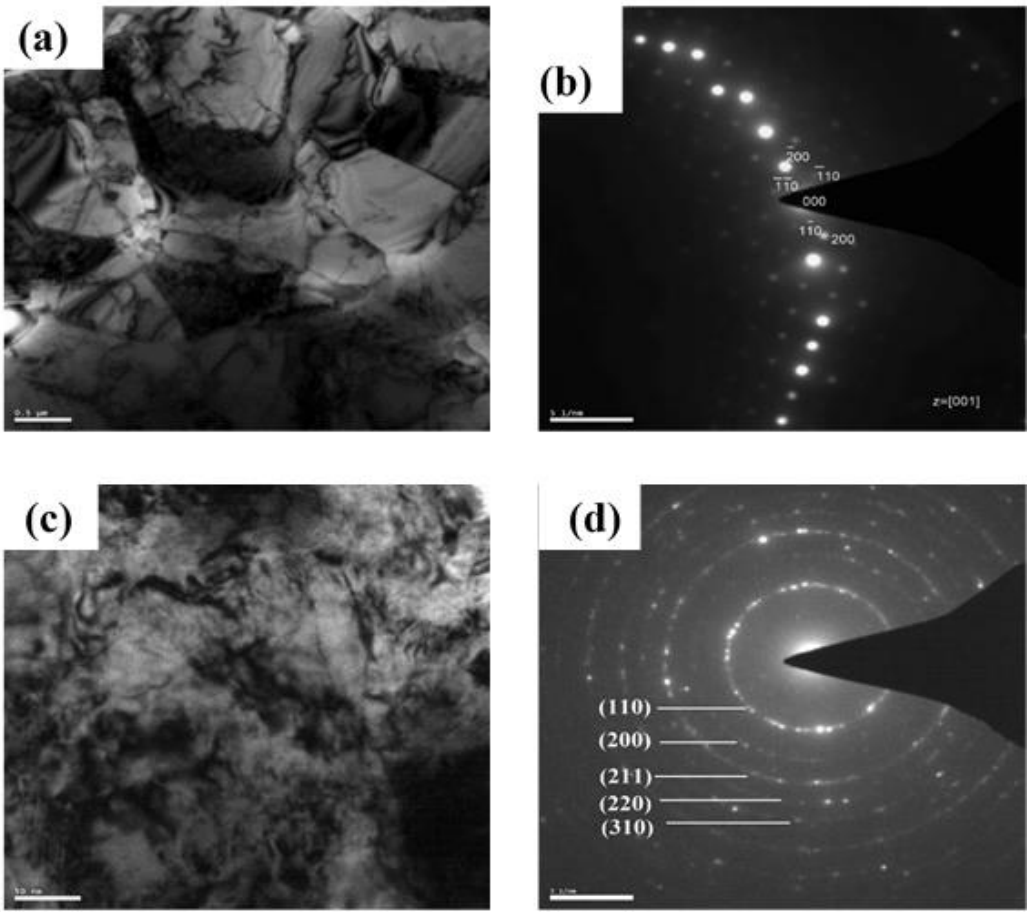

Figure 9. TEM micrographs of type AISI 446SS **(a, b)** Non-USPed, and **(c, d)** 2min USPed. [*Reprinted from* Mishra et al., 2020, Engineering Failure Analysis, 118, 104873 *with permission from* Elsevier].

4. Hot Corrosion-Erosion Resistance By Surface Nanostructuring

The combined effect of hot corrosion-erosion is achieved by forming nanostructured grains on the surface. To fulfil the purpose, a novel technique of ultrasonic shot peening is used. This technique caused grain refinement of ≤ 65nm to a depth of ~ 250 μm and led to the improvement of hot-corrosion resistance of Type AISI 446SS. This is due to high diffusivity of chromium on the surface from the alloy and formed a high corrosion resistance layer of Cr_2O_3 on the surface Figure 10. This can be verified from the weight gain of the specimens under hot corrosion test where the gain is significant in case of un-shot peened samples as compared to that with shot peened samples. The USP not only modifies the grain structure, but also significantly contributes to increase the surface roughness. The impact of hardened steel balls induces severe plastic deformation on the surface of the alloy but the material does not undergo any phase change. This grain refinement under USP can be seen as peak broadening in XRD pattern. Surface modification by USP treatment led to large-scale grain refinement, forming nano grains on the surface and thus the consistency of grain boundary increases. This increase in grain boundary facilitates the diffusion of chromium from the bulk towards the surface of the alloy, and thereby forming a thick protective layer of chromia i.e., Cr_2O_3. This Cr_2O_3 layer covers the grain boundaries and led to decrease the activity of oxygen on the treated surface, resulting in enhancement of corrosion resistance (Arabnejad et al., 2015).

Later, when these hot corroded samples are subjected to erosion test, they suffer severe loss of the material by striking the surface and transforming their kinetic energy to cause deformation. The high velocity impacting steel balls generate plastic deformation and create dimples over the surface, causing increased surface roughness. The process of material removal takes place from the corroded layer as well as from the SNC layer.

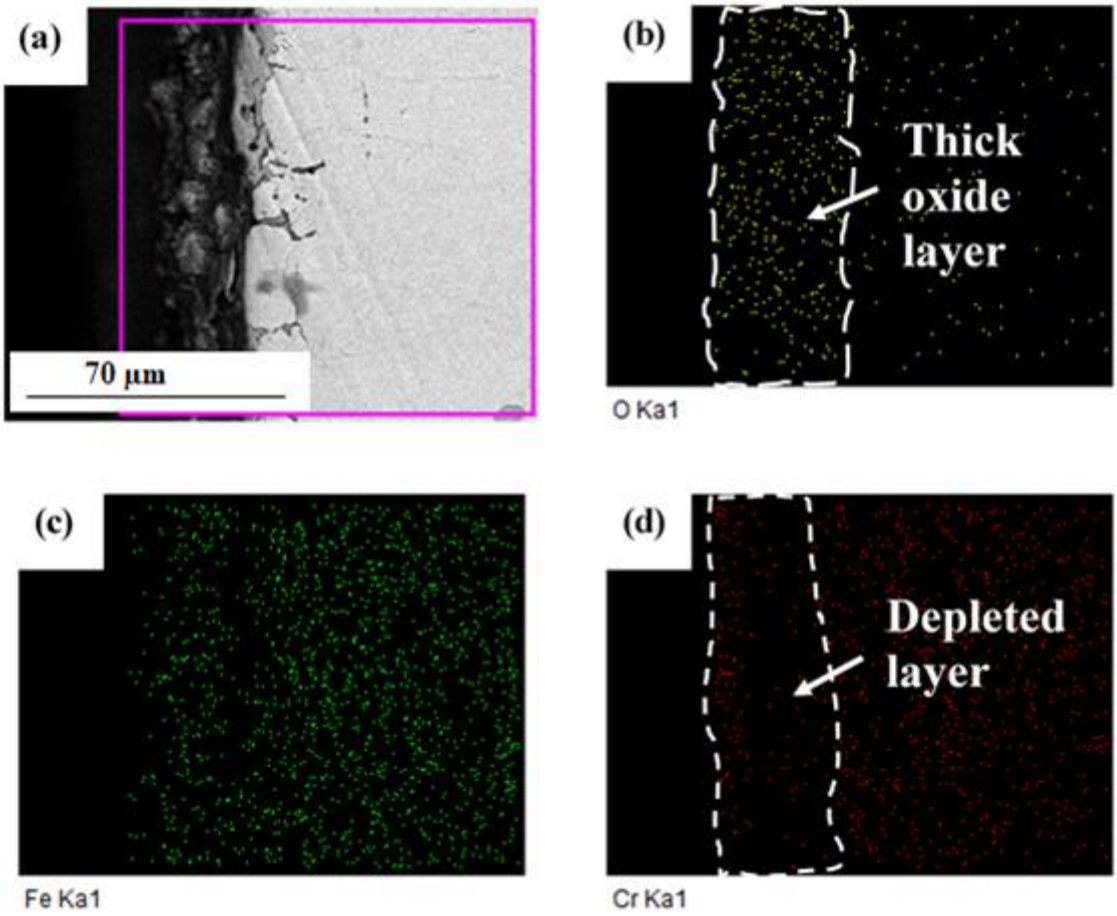

Figure 10. Cross sectional X-ray mapping of the salt mixture deposited 2min USPed sample exposed at 650℃ for 20 h, focussing the elemental distribution (a) cross-section, (b) Oxygen, (c) Iron, (d) Chromium [*Reprinted from* Mishra et al., 2020, Engineering Failure Analysis, 118, 104873 *with permission from* Elsevier].

5. Summary

Ferritic stainless steel grade is a low maintenance alloy that finds extensive applications in power plants, chemical industries, exhaust manifolds, etc. These alloys are cost effective over various other grades of steel. The application of ferritic stainless steels is gaining popularity due to their physical, chemical and mechanical properties. Along with, they also have strong corrosion and oxidation resistance, and excellent resistance to crevice, pitting and stress corrosion cracking. These properties makes the material viable to certain corrosion applications like heat exchangers, food industries and architectural trims, etc. The pipelines of the heat exchangers during their operation and maintenance undergo hot corrosion-erosion due to salt present in the flowing fluid. The presence of salt in high-temperature conditions causes hot corrosion, which degrades the material surface and advances the erosion rate. Surface modification is the most

promising route to enhance the erosion-corrosion behavior of materials substrate. Several processes of surface modifications and microstructure development, like, severe plastic deformation, surface coatings, ball milling, shot peening, friction stir processing, LSP and USP takes the advantage to intensify the surface properties of the structural component. In this legacy, a novel approach of surface nanostructuring had been effectively utilised by using ultrasonic shot peening in ferritic stainless steel (Type AISI 446SS) towards enhancing the hot corrosion-erosion resistance.

Conflict of Interest

The authors declare that they have no known competing financial interests or personal relationships that could appear to have influenced the work reported in this paper.

Acknowledgements

The authors are very grateful to the PMSL for according permission to include my article in this book. We sincerely thank the editors for their untiring efforts to help in preparing this manuscript.

References

Arabnejad, H., Shirazi, S.A., McLaury, B.S., Subramani, H.J., & Rhyne, L.D. (2015). The effect of erodent particle hardness on the erosion of stainless steel. *Wear*, *332*, 1098-1103.

Balakrishnan, A., Lee, B.C., Kim, T.N., & Panigrahi, B.B. (2008). Corrosion behaviour of ultra fine grained titanium in simulated body fluid for implant application. *Trends in Biomaterials & Artificial Organs*, *22*(1), 58-64.

Bao, L., Li, K., Zheng, J., Zhang, Y., Zhan, K., Yang, Z., Zhao, B., & Ji, V. (2022). Surface characteristics and stress corrosion behavior of AA 7075-T6 aluminum alloys after different shot peening processes. *Surface and Coatings Technology*, *440*, 128481.

Charles, J., Mithieux, J.D., Santacreu, P.O., & Peguet, L. (2009). The ferritic stainless family: The appropriate answer to nickel volatility?. *Revue de Métallurgie*, *106*(3), 124-139.

Chen, C., & Zhang, H. (2021). Characteristics of friction and wear of Al-Zn-Mg-Cu alloy after application of ultrasonic shot peening technology. *Surface and Coatings Technology*, *423*, 127615.

Chen, G.Q., Yan, J.I.A.O., Tian, T.Y., Zhang, X.H., Li, Z.Q., & Zhou, W.L. (2014). Effect of wet shot peening on Ti-6Al-4V alloy treated by ceramic beads. *Transactions of Nonferrous Metals Society of China*, *24*(3), 690-696.

Chen, H., Guan, Y., Zhu, L., Li, Y., Zhai, J., & Lin, J. (2021). Effects of ultrasonic shot peening process parameters on nanocrystalline and mechanical properties of pure copper surface. *Materials Chemistry and Physics*, *259*, 124025.

Chen, X., Xie, X., Zhang, Y., Wang, H., & Liang, Z. (2023). Tungsten carbide coating prepared by ultrasonic shot peening to improve the wear properties of magnesium alloys. *Journal of Materials Research and Technology*, *26*, 2451-2464.

Chung, R.J., Jiang, J., Pang, C., Yu, B., Eadie, R., & Li, D.Y. (2021). Erosion-corrosion behaviour of steels used in slurry pipelines. *Wear*, *477*, 203771.

Chung, R.J., Jiang, J., Pang, C., Yu, B., Eadie, R., & Li, D.Y. (2023). Erosion-corrosion behaviour of high manganese steel used in slurry pipelines. *Wear*, 204885.

Dwivedi, P.K., Sivateja, C., Rai, A.K., Ganesh, P., Basu, A., & Dutta, K. (2023). A comparative assessment of the effects of laser shock peening and ultrasonic shot peening on surface integrity and ratcheting fatigue performance of HSLA steel. *International Journal of Fatigue*, *176*, 107902.

Fragoudakis, R., Saigal, A., Savaidis, G., Malikoutsakis, M., Bazios, I., Savaidis, A., & Karditsas, S. (2013). Fatigue assessment and failure analysis of shot-peened leaf springs. *Fatigue & Fracture of Engineering Materials & Structures*, *36*(2), 92-101.

Hancock, P. (1987). Vanadic and chloride attack of superalloys. *Materials Science and Technology*, *3*(7), 536-544.

Koul, A.K., & Castillo, R. (1993). Creep Bahavior of Industrial Turbine Blade Materials. *Proceeding of ASM Materials Congress* (75-88) Pittsburgh, Pennsylvania.

Kubaschewski, O. (2013). *Iron—Binary phase diagrams*. Springer Science & Business Media.

Kumar, N., Das, A., Sarkar, S., & Arora, N. (2023). Improving erosion resistance through solution treatment of nitronic and martensitic steels for slurry erosive applications. *Wear*, *530*, 205060.

Kumar, S., Chattopadhyay, K., Mahobia, G.S., & Singh, V. (2016). Hot corrosion behaviour of Ti–6Al–4V modified by ultrasonic shot peening. *Materials & Design*, *110*, 196-206.

Kumar, S., Mishra, A., Mohan, S., & Mahobia, G.S. (2021). The solid particle erosion of pre oxidized high manganese nitrogen stabilized austenitic stainless steel (18Cr-21Mn-0.65 N-Fe) at 400 to 700° C. *Surface Topography: Metrology and Properties*, *9*(3), 035002.

Kumar, S., Rao, G.S., Chattopadhyay, K., Mahobia, G.S., Srinivas, N.S., & Singh, V. (2014). Effect of surface nanostructure on tensile behavior of superalloy IN718. *Materials & Design (1980-2015)*, *62*, 76-82.

Lee, H.S., Kim, D.S., Jung, J.S., Pyoun, Y.S., & Shin, K. (2009). Influence of peening on the corrosion properties of AISI 304 stainless steel. *Corrosion Science*, *51*(12), 2826-2830.

Li, Y., Burstein, G.T., & Hutchings, I.M. (1995). The influence of corrosion on the erosion of aluminium by aqueous silica slurries. *Wear*, *186*, 515-522.

Liu, G., Lu, J., & Lu, K. (2000). Surface nanocrystallization of 316L stainless steel induced by ultrasonic shot peening. *Materials Science and Engineering: A*, *286*(1), 91-95.

McCabe, L.P., Sargent, G.A., & Conrad, H. (1985). Effect of microstructure on the erosion of steel by solid particles. *Wear*, *105*(3), 257-277.

Mishra, A. (2019). *High temperature solid particle erosion of type 446 stainless steel* (Doctoral dissertation, IIT BHU).

Mishra, A., Behera, C.K., Mohan, S., Mohan, A., & Pradhan, D. (2020). High temperature erosion behaviour of Type AISI 446 stainless steel under the combined effect of surface modification and pre hot-corrosion. *Engineering Failure Analysis*, *118*, 104873.

Mishra, R., & Balasubramaniam, R. (2004). Effect of nanocrystalline grain size on the electrochemical and corrosion behavior of nickel. *Corrosion Science*, *46*(12), 3019-3029.

Oka, Y.I., Ohnogi, H., Hosokawa, T., & Matsumura, M. (1997). The impact angle dependence of erosion damage caused by solid particle impact. *Wear*, *203*, 573-579.

Pandey, V. (2018). *Effect of ultrasonic shot peening on microstructure, low cycle fatigue and corrosion behaviour of AA7075 aluminium alloy* (Doctoral dissertation).

Peltz, J.D.S., Antonini, L.M., Kunst, S.R., Ludwig, G.A., Fuhr, L.T., & Malfatti, C.D.F. (2014). Effect of application of the shot peening process in the corrosion resistance of the AISI 430 ferritic stainless steel. In *Materials Science Forum* (Vol. 775, pp. 365-369). Trans Tech Publications Ltd.

Pradhan, D., Mahobia, G.S., Chattopadhyay, K., & Singh, V. (2018). Effect of surface roughness on corrosion behavior of the superalloy IN718 in simulated marine environment. *Journal of Alloys and Compounds*, *740*, 250-263.

Prakash, S. (2008). Hot corrosion of alloys and coatings. In *Developments in High Temperature Corrosion and Protection of Materials* (pp. 164-191). Woodhead Publishing.

Qin, Z., Li, B., Chen, T., Chen, C., Chen, R., Ma, H., Xue, H.., Yao, C., & Tan, L. (2023). Comparative study of the effects of conventional shot peening and ultrasonic shot peening on very high cycle fatigue properties of GH4169 superalloy. *International Journal of Fatigue*, *175*, 107799.

Rai, P.K., Pandey, V., Chattopadhyay, K., Singhal, L.K., & Singh, V. (2014). Effect of ultrasonic shot peening on microstructure and mechanical properties of high-nitrogen austenitic stainless steel. *Journal of Materials Engineering and Performance*, *23*, 4055-4064.

Reck, B.K., Chambon, M., Hashimoto, S., & Graedel, T.E. (2010). Global stainless steel cycle exemplifies China's rise to metal dominance. *Environmental Science & Technology*, *44*(10), 3940-3946.

Rehaman, S., Kushwaha, A., & Basu, A. (2023). Effect of ultrasonic shot peening on electrodeposited Ni and Cu coatings on Cu substrate. *Materials Today: Proceedings*, *91*(1), 95-102.

Roland, T., Retraint, D., Lu, K., & Lu, J. (2006). Fatigue life improvement through surface nanostructuring of stainless steel by means of surface mechanical attrition treatment. *Scripta Materialia*, *54*(11), 1949-1954.

Sandá, A., Navas, V.G., & Gonzalo, O. (2011). Surface state of Inconel 718 ultrasonic shot peened: Effect of processing time, material and quantity of shot balls and distance from radiating surface to sample. *Materials & Design*, *32*(4), 2213-2220.

Sun, H.Q., Shi, Y.N., Zhang, M.X., & Lu, K. (2007). Plastic strain-induced grain refinement in the nanometer scale in a Mg alloy. *Acta Materialia*, *55*(3), 975-982.

Sundararajan, G., & Roy, M. (1997). Solid particle erosion behaviour of metallic materials at room and elevated temperatures. *Tribology International*, *30*(5), 339-359.

Tan, L., Ren, X., Sridharan, K., & Allen, T.R. (2008). Effect of shot-peening on the oxidation of alloy 800H exposed to supercritical water and cyclic oxidation. *Corrosion Science*, *50*(7), 2040-2046.

Tao, N. R., Lu, J., & Lu, K. (2008, June). Surface nanocrystallization by surface mechanical attrition treatment. In Materials science forum (Vol. 579, pp. 91-108). Trans Tech Publications Ltd. https://doi.org/10.4028/www.scientific.net/msf.579.91.

Wang, F., Xu, W., Huang, H., Li, C.C., & Chen, L.Q. (2022a). Investigation on Erosion-Corrosion Behavior of Q235 Steel in Liquid-Solid Flow Using Electrochemical Method and Numerical Simulation. *International Journal of Electrochemical Science*, *17*(11), 221184.

Wang, K., Tao, N.R., Liu, G., Lu, J., & Lu, K. (2006). Plastic strain-induced grain refinement at the nanometer scale in copper. *Acta Materialia*, *54*(19), 5281-5291.

Wang, L., Lin, Y., Zeng, Z., Liu, W., Xue, Q., Hu, L., & Zhang, J. (2007). Electrochemical corrosion behavior of nanocrystalline Co coatings explained by higher grain boundary density. *Electrochimica Acta*, *52*(13), 4342-4350.

Wang, W., Hu, J., Yuan, X., Zhou, L., Yu, J., Zhang, Z., & Zhong, X. (2022b). Understanding the effect of tensile stress on erosion-corrosion of X70 pipeline steel. *Construction and Building Materials*, *342*, 127972.

Wang, Z.B., Lu, J., & Lu, K. (2005). Chromizing behaviors of a low carbon steel processed by means of surface mechanical attrition treatment. *Acta Materialia*, *53*(7), 2081-2089.

Wang, Z.B., Tao, N.R., Tong, W.P., Lu, J., & Lu, K. (2003). Diffusion of chromium in nanocrystalline iron produced by means of surface mechanical attrition treatment. *Acta Materialia*, *51*(14), 4319-4329.

Yang, Z., Zheng, J., Zhan, K., Jiang, C., & Ji, V. (2022). Surface characteristic and wear resistance of S960 high-strength steel after shot peening combing with ultrasonic sprayed graphene oxide coating. *Journal of Materials Research and Technology*, *18*, 978-989.

Yue, T.M., Yu, J.K., Mei, Z., & Man, H.C. (2002). Excimer laser surface treatment of Ti–6Al–4V alloy for corrosion resistance enhancement. *Materials Letters*, *52*(3), 206-212.

Yue, X., Hu, S., Wang, X., Liu, Y., Yin, F., & Hua, L. (2022). Understanding the nanostructure evolution and the mechanical strengthening of the M50 bearing steel during ultrasonic shot peening. *Materials Science and Engineering: A*, *836*, 142721.

Zhang, H.W., Hei, Z.K., Liu, G., Lu, J., & Lu, K. (2003). Formation of nanostructured surface layer on AISI 304 stainless steel by means of surface mechanical attrition treatment. *Acta Materialia*, *51*(7), 1871-1881.

Zheng, Y., Yao, Z., Wei, X., & Ke, W. (1995). The synergistic effect between erosion and corrosion in acidic slurry medium. *Wear*, *186*, 555-561.

Zhu, K.Y., Vassel, A., Brisset, F., Lu, K., & Lu, J. (2004). Nanostructure formation mechanism of α-titanium using SMAT. *Acta Materialia*, *52*(14), 4101-4110.